# Modified Nb-Si-Based Multi-Element Alloys

Subjects: Biochemical Research Methods

Contributor: Yingyi Zhang

Nb-Si-based superalloys are considered as the most promising high-temperature structural material to replace the Ni-based superalloys. Unfortunately, the poor oxidation resistance is still a major obstacle to the application of Nb-Si-based alloys. Alloying is a promising method to overcome this problem.

microstructure alloying Nb-Si Modification

## 1. Nb-Si-Based Alloys Modified with Hf Elements

In order to promote the high-temperature oxidation resistance of Nb-Si-based alloys, researchers have tried to add different kinds of elements, and Hf is a common addition element. Geng et al. [1] produced the Nb-Si-Al-Cr alloy by a non-consumption arc-melting process and the effects of Ti, Mo, and Hf on the oxidation behavior of the alloy at different temperatures were studied. **Figure 1** shows cross-sections of the oxidized alloys. The scales of the alloy were a complex mixture of Nb and Ti oxides; oxygen was dissolved in the niobium solid solution (Nbss) below the oxide scale of the alloy. The oxidation kinetics curve is shown in **Figure 2**a. It can be seen that the oxidation of these alloys includes two stages: the initial linear stage and the later parabolic stage. The weight gain rate of the alloy with the Hf element decreases gradually after 55 h of oxidation, while its oxidation resistance becomes worse after heat treatment. Furthermore, Geng et al. [2] have also studied the effects of Ti, Hf, and Sn on the oxidation resistance of the Nb-Si-Al-Cr-Mo alloy, and the oxidation weight gain curve is shown in **Figure 2**b. It is clear that the addition of Hf decreases the oxidation rate of as-cast alloy but increases the oxidation rate of heat-treated alloy. The oxidation behavior of these alloys is mainly controlled by the oxidation of Nbss, and the volume fraction of Nbss has a great impact on the oxidation resistance of the alloy.

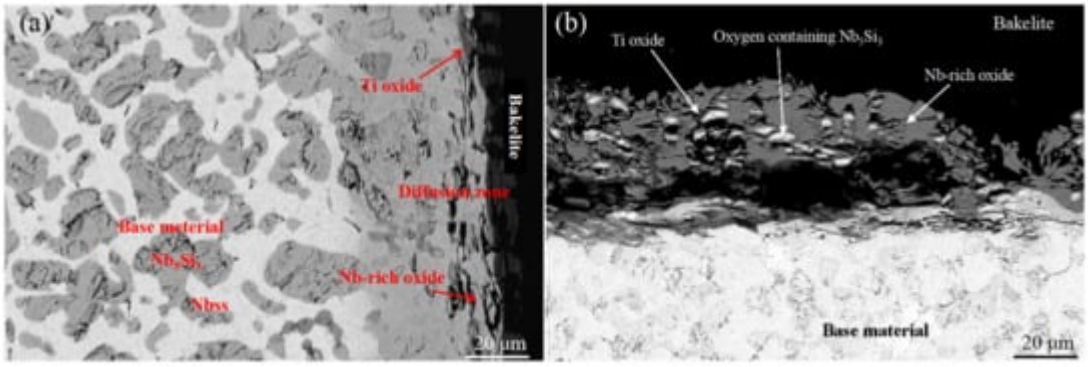


**Figure 1.** BSE images of the microstructures of cross-sections of the (**a**) Nb-24Ti-18Si-5Al-5Cr-2Mo and (**b**) Nb-24Ti-18Si-5Al-5Cr-2Mo-5Hf after oxidation at 800 °C. Copyright 2006 Elsevier.

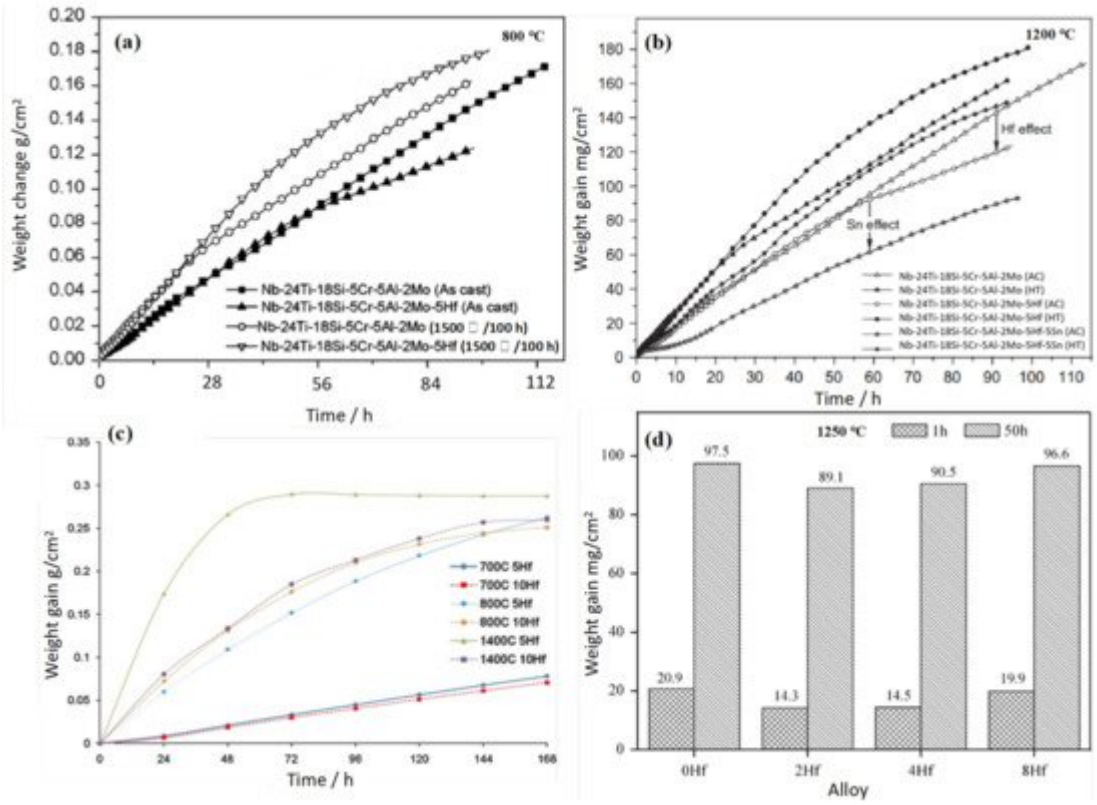


**Figure 2.** Weight change curves of Nb-Si-based alloys with Hf addition oxidized at (**a**) 800 °C and (**b**) 1200 °C. (**c**) Cyclic oxidation curves for Nb-20Si-20Cr-(5, 10 at.%) Hf alloys. (**d**) Oxidation weight gain histogram of Nb-22Ti-16Si-3Cr-Al-2B-xHf (x = 0 at.%, 2 at.%, 4 at.%, 8 at.%) alloys at 1250 °C. Copyright 2006 Elsevier, 2011 Elsevier and 2015 Elsevier.

In addition, Vazquez et al. [3] also studied the effects of Hf element on the antioxidant properties of Nb-Si-based alloys. The microscopic morphology of the alloy after oxidation is shown in **Figure 3**. Analysis shows that the products of oxidation are $Nb_2O_5$, $HfO_2$, and un-reacted $NbCr_2$. Nbss in the alloy is prone to selective oxidation. After long-term oxidation at 700 °C, there are a large number of powder oxides and cracks in the oxide layer, which has no protective effect. **Figure 2**c shows the oxidation curves for both alloys doped with 5Hf and 10Hf (at.%) at 700, 800, and 1400 °C, respectively. The oxidation experiments reveal that both alloys exhibit a good oxidation resistance at 700 °C, the 10Hf alloy has lower oxidation weight gain than 5Hf alloy at all temperatures. The researchers attribute the alloy's better oxidation resistance to the formation of a thin protective layer.

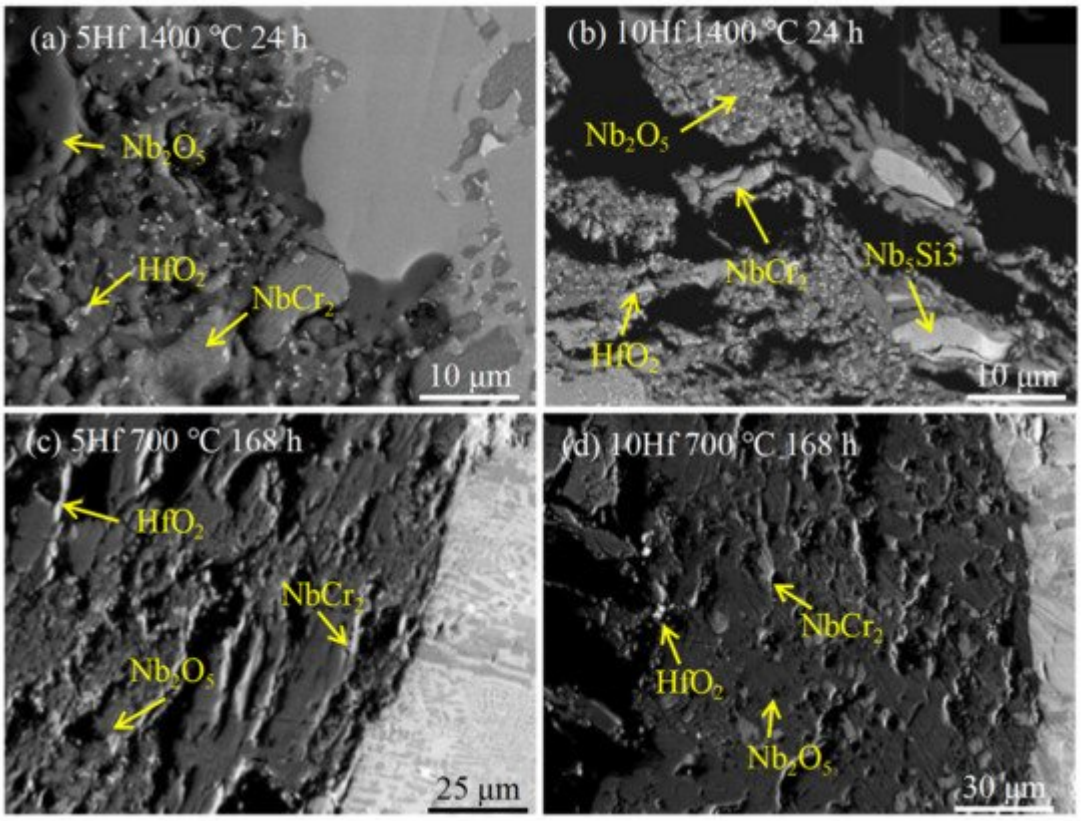


**Figure 3.** Microstructure of Nb-20Cr-20Si-5Hf alloy (**a**,**c**) and Nb-20Cr-20Si-10Hf alloy (**b**,**d**) after short-term oxidation at 1400 °C and long-term oxidation at 700 °C. Copyright 2011 Elsevier.

Zhang et al. [4] studied the effects of Hf, B, and Cr on the antioxidant properties of Nb-Si-based superalloys. The research shows that the weight gain per unit area of the alloy decreases from 157 to 139 mg/cm$^2$ after oxidation at 1250 °C for 50 h. Meanwhile, the synergistic addition of Hf, B, and Cr makes the oxidation resistance of the alloy more excellent. Zhang et al. [5]. also studied the antioxidant properties of Nb-Si-based alloys with different Hf contents and found that the oxide layers of these alloys fell off and had poor adhesion. The cross-sectional BSE image of the alloy after oxidation is shown in **Figure 4**. The oxides of the alloys are $TiO_2$ and $HfO_2$, as determined by EDS. $HfO_2$ is mainly found at the interface between Nbss and $(Nb,X)_5Si_3$ (rod-like morphology) or at the edges of silicide blocks (needle-like morphology). More severe internal oxidation occurs with Hf addition. With the addition of Hf, the formation of α$(Nb,X)_5Si_3$ was inhibited, while the formation of γ$(Nb,X)_5Si_3$ was promoted, and the former has better oxidation resistance, since the former phase is not attacked, while the latter phase is partly oxidized. The histogram of oxidation weight gain is shown in **Figure 2**d. It is obvious that the weight change of the alloy decreases first and then increases with the increase in Hf, and the alloy with 2Hf (at.%) has the least weight gain. It may be due to the large size of Hf atoms, which inhibited the diffusion of other metal atoms. Although the addition of 8Hf (at.%) did not improve the oxidation resistance of the alloy, it increased the room temperature fracture toughness of the alloy, and the eutectic structure in the alloy has been refined significantly. It can be seen that the contents of Hf have a great influence on the comprehensive performance of the alloy.

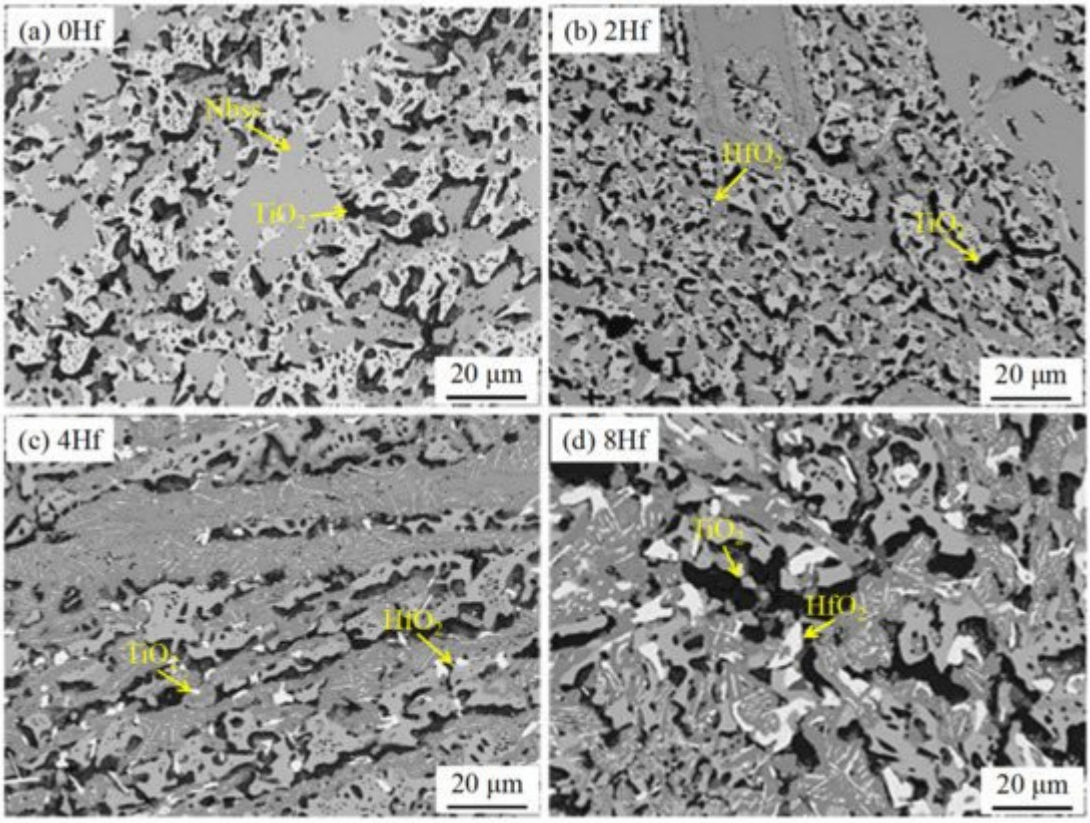


**Figure 4.** Cross-sectional BSE images of the internal oxidation zones of the Nb-22Ti-16Si-3Cr-3Al-2B-xHf. (x = 0 at.%, 2 at.%, 4 at.%, 8 at.%) alloys upon oxidation at 1250 °C for 50 h.(**a**) 0Hf alloy. (**b**) 2Hf alloy. (**c**) 4Hf alloy. (**d**) 8Hf alloy. Copyright 2015 Elsevier.

## 2. Nb-Si-Based Alloys Modified with Cr Elements

Chromium has the advantages of high melting point, excellent chemical stability, and easy alloying with other elements. It is widely used in Fe-based and Ni-based alloys. The $Cr_2Nb$ phase formed after the addition of Cr element in niobium alloy has the advantages of high melting point and oxidation resistance [6][7][8]. The oxide $CrNbO_4$ has better oxidation resistance than $Nb_2O_5$, and it can also improve the adhesion between the oxide layer and substrate [9][10]. Zhang et al. [4] studied the effects of Hf, B, and Cr elements on the microstructure and properties of Nb-Si-based superalloys by a vacuum non-consumption arc-melting process. (The alloy with x at.% Hf, y at.% B, and z at.% Cr content is denoted by xHf-yB-zCr below.) The histogram of the oxidation weight gain of alloys with different compositions is shown in **Figure 5**a. Obviously, the 0Hf-0B-0Cr alloy (base alloy) has the most weight gain after oxidation (157 mg/cm$^2$ for 50 h), displaying the worst oxidation resistance. The oxidation weight gain decreases from 157 to 139 mg/cm$^2$ after Hf addition (4Hf-0B-0Cr alloy), and the oxidation resistance is slightly ameliorated. Furthermore, the synergistic effects of Hf, Cr, and B enhance the oxidation resistance of the alloy significantly, and the weight gain of the 4Hf-2B-5Cr alloy is 91 mg/cm$^2$ at 50 h. The room temperature fracture toughness of the alloy decreases with the addition of Cr, and the microhardness increases with the addition of Cr. In addition, Wang et al. [9] prepared the Nb-22Ti-14Si-2HF-2Al-xCr (x = 2 at.%, 6 at.%, 10 at.%, 14 at.%, 17 at %) alloys, and the effect of Cr on oxidation resistance and mechanical properties of the alloy were studied. **Figure 5**b

shows the oxidation kinetics curve of these alloys at 1250 °C. It is obvious that with the increase in the contents of Cr, the oxidation weight gain decreases gradually, and the oxidation resistance of the alloy improves gradually. The 17Cr (at.%) alloy has the best antioxidant properties, which may be due to the formation of the protective $Cr_2O_3/SiO_2$ film. In addition, with the increase in Cr content, the fracture toughness of the alloy decreases, and the hardness of Nbss increases. Moreover, the studies of Zelenitsas [11] and Esparza [12] show that the synergy of Cr and Al can form the protective $Al_2O_3/CrNbO_4$ film and reduce the oxidation rate inside the alloy. The Cr element has stronger O affinity than Nb, and the formation of stable $Cr_2O_3$ can improve the compactness and stability of the oxide layer [13][14][15]; thus, the alloy has better oxidation resistance.

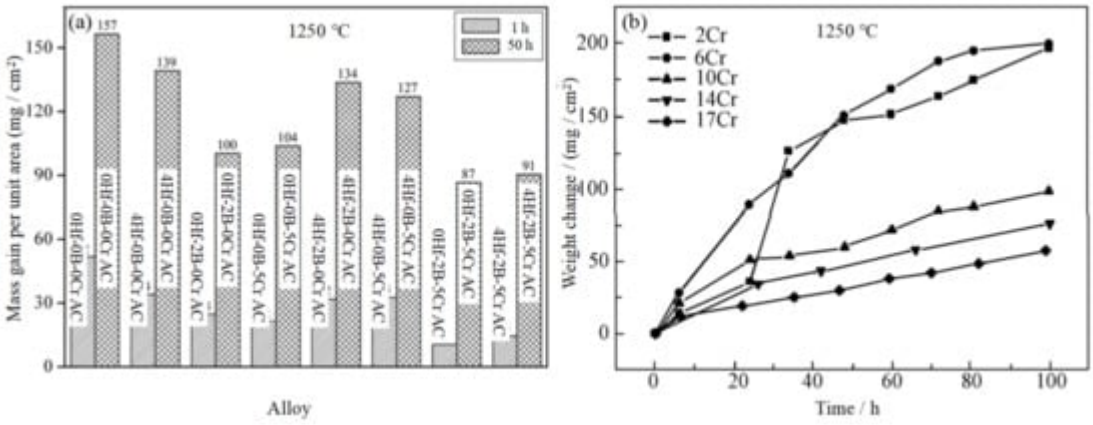


**Figure 5.** (**a**) Oxidative weight gain histogram of the Nb-Si-based alloys oxidized at 1250 °C. (**b**) The oxidation weight gain curve of Nb-Si alloy with different Cr content at 1250 °C. Copyright 2012 Elsevier and 2015 Elsevier.

## 3. Nb-Si-Based Alloys Modified with Zr Elements

Among the many types of alloy systems, Zr addition can refine the microstructure and promote the oxidation resistance of the alloy [16][17][18][19]. After the oxidation of Zr, $ZrO_2$ is formed, which has the characteristics of low thermal conductivity, excellent thermal vibration resistance, and oxidation resistance. In the work of Zhang et al. [20], the effect of V, Zr, and other elements on the antioxidant properties of Nb-15Si-24Ti-4Cr-2Al-2Hf (at %) alloy was investigated. The surface SEM images of the alloy oxide upon 1250 °C for 100 h are shown in **Figure 6**a–c; **Figure 6**(a1–c1) show the macroscopic morphology after oxidation. It is apparent that the alloy has a rough and porous surface, and the oxide layer is seriously peeled off. The condition has not been improved after adding V, but the oxide layer is relatively dense and complete after adding Zr. **Figure 6**d–f shows the SEM morphology of the oxidation cross-section, and the oxide layer consists of inner and outer layers. The surface of the base alloy and 1 V alloy after oxidation is loose and porous after peeling off. Although the oxide layer of 1Zr alloy falls off also, an oxide layer rich in silicon and oxygen is formed on the surface. Combined with the oxidation kinetics curve in **Figure 7**a, it can be inferred that a protective oxide layer is produced on the surface of the 1Zr alloy. The results of WDS and EPMA analysis show that an $SiO_2$ film is formed in the oxide outer layer, which inhibits the diffusion of $O_2$ and protects the alloy substrate.

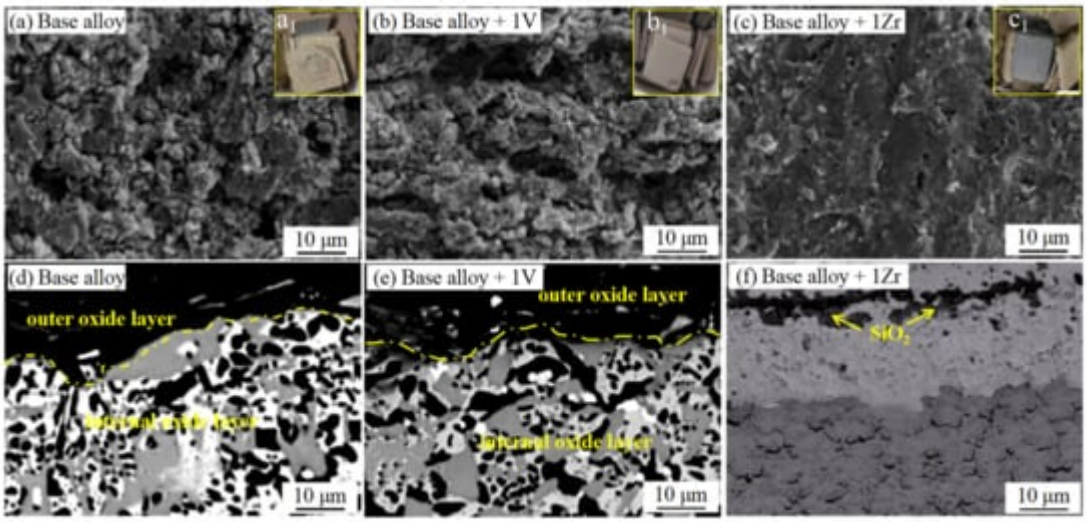


**Figure 6.** Surface SEM images of Nb-Si-based alloys after oxidation at 1250 °C for 100 h: (**a**) base alloy, (**b**) 1V alloy, (**c**) 1Zr alloy. a1–c1 are the corresponding macroscopic morphology. Cross-sectional SEM images of Nb-Si-based alloys after oxidation: (**d**) base alloy, (**e**) 1 V alloy, (**f**) 1Zr alloy. Copyright 2017 Springer Nature.

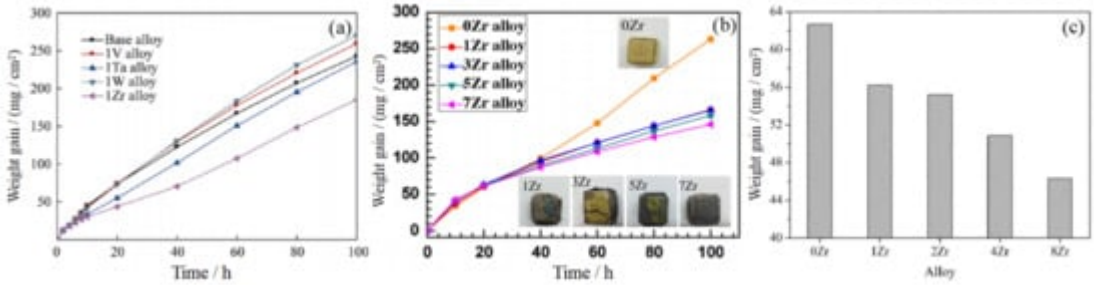


**Figure 7.** Weight gain versus time for Nb-Si-based alloys oxidized at 1250 °C for 100 h (**a**). Oxidation weight gain curve (**b**) and oxidation weight gain histogram (**c**) of Nb-Si-based alloys with different Zr contents. Copyright 2017 Springer Nature, 2019 Elsevier and 2017 Elsevier.

In order to ascertain the influence of Zr content on the oxidation resistance of Nb-Si-based alloy, Zhang et al. [21] designed the Nb-Si-based alloys with different Zr content, and the oxidation behavior of the alloy at 1300 °C was studied. The microstructure of the oxide layer on the alloy surface is shown in **Figure 8**a–d. It is apparent that the oxide on the surface of 0Zr and 3Zr alloys is rod-like, rough, and porous. When the Zr content reaches more than 5 at.%, the oxides have a polygonal structure and compact arrangement. **Figure 8**e–h show the oxidation fracture surface microstructures of 0Zr, 3Zr, 5Zr, and 7Zr, respectively, and the oxide layer is mainly composed of $TiO_2$, $Nb_2O_5$, $TiNb_2O_7$, and $Ti_2Nb_{10}O_{29}$. A small amount of $ZrO_2$ is detected in the 7Zr alloy. Meanwhile, no $SiO_2$ is detected in the oxide, which may be attributed to the amorphous state of $SiO_2$. **Figure 7**b shows the oxidation kinetics curve of the alloy. It is obvious that the weight gain of the alloy decreases with the increase in Zr. The weight gain curves of 1Zr and 3Zr alloys almost coincide, while the weight gain of 7Zr alloy is about 44% lower than that of 0Zr alloy. Combined with the macroscopic morphology of these alloys after oxidation, it can be seen that the 7Zr alloy has the best oxidation resistance.

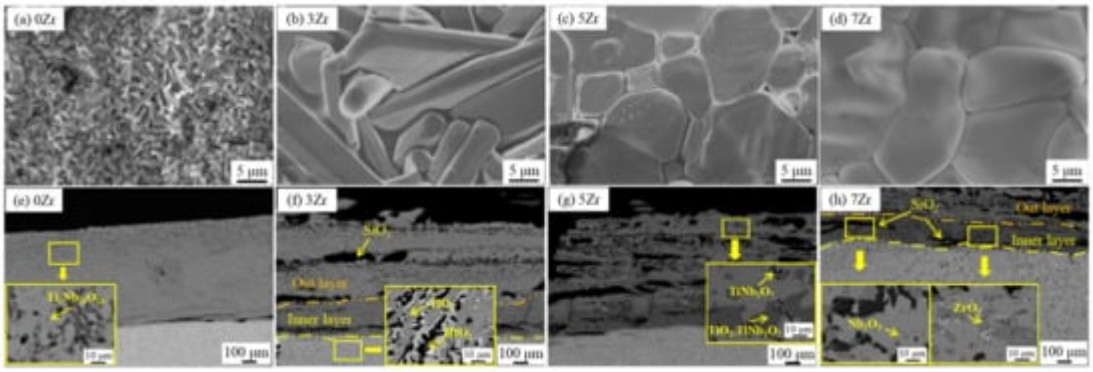

**Figure 8.** Surface morphologies and cross-sectional microstructures of Nb-15Si-24Ti-4Cr-2Al-2Hf-xZr (x = 0 at.%, 3 at.%, 5 at.%, 7 at.%) alloys after oxidation at 1300 °C for 100 h. (**a**,**e**) 0Zr; (**b**,**f**) 3Zr; (**c**,**g**) 5Zr; (**d**,**h**) 7Zr. Copyright 2019 Elsevier.

In addition, Qiao et al. [22] also carried out a similar study on the effect of Zr content on the microstructure and properties of Nb-Si-based alloys. **Figure 9** shows the cross-section BSE image of the alloy after oxidation at 1250 °C for 20 h. It is evident that there are many cracks and holes in the oxide layer, and the thickness of the oxide layers ranges from 260 to 380 μm. The EPMA-WDS analysis shows that the phase composition of the outer layer is $TiNb_2O_7$ and $TiO_2$, and the inner layer is $Ti_2Nb_{10}O_{29}$ and $Nb_2O_5$. In addition, $ZrO_2$ was also detected in the scales of 4Zr and 8Zr alloys. Obviously, the weight gain of the sample decreases with the increase in Zr, as shown in **Figure 7**c. It can be seen that Zr plays an important role in advancing the antioxidant properties of Nb-Si-based alloys; meanwhile, the addition of Zr improves not only the room-temperature fracture toughness but also the high-temperature strength and compressive strength of the alloy. In addition, Ma et al. [23] showed that adding Zr or V alone can improve the oxidation resistance of Nb-Si series alloys, but the simultaneous addition of Zr and V will form the $CrVNbO_6$/$VNb_9O_{25}$ harmful oxides, which will reduce the service time of Nb-Si alloys. Moreover, the addition of Zr improves the room-temperature fracture toughness and compressive yield strength of the alloy, and the phase microhardness is also improved due to the solution strengthening effect of Zr.

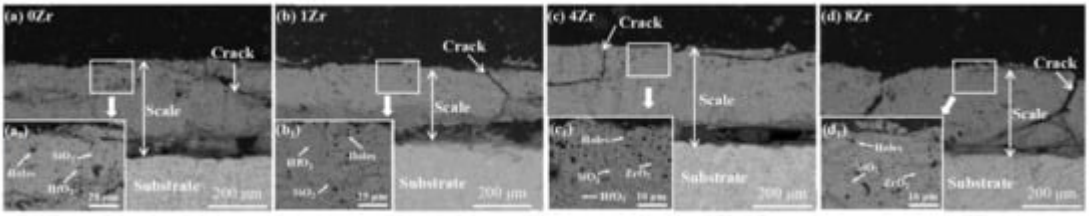

**Figure 9.** Cross-sectional BSE images of the Nb-22Ti-15Si-5Cr-3HF-3Al-xZr (x = 0 at.%, 1 at.%, 4 at.%, 8 at %) alloys after oxidation at 1250 °C for 20 h. (**a**) 0Zr; (**b**) 1Zr; (**c**) 4Zr; (**d**) 8Zr. The $a_1$, $b_1$, $c_1$, and $d_1$ are microarea images in figures (**a**–**d**), respectively. Copyright 2017 Elsevier.

## 4. Nb-Si-Based Alloys Modified with B Elements

B elements can refine the grain size and improve the toughness of materials. Studies have shown that the borosilicate glassy layer formed by B and Si in Mo-Si-B alloys has a good repairing effect on cracks and holes in oxide scales [24][25][26][27][28][29], which is of great significance to ameliorate the comprehensive properties. Zhang et al. [28] prepared the Nb-22Ti-16Si-5Cr-4Hf-3Al alloy with different contents of B and studied the effect of B on the microstructure and properties of the alloy. The layer is composed of $TiNb_2O_7$, (Ti, Nb, Cr)$O_2$, and Si, as shown in **Figure 10**. Unexpectedly, no silicon oxide was detected in the oxide layer, which may be due to the formation of amorphous silicate. The oxidation weight gain of 0B, 2B, and 5B alloys are 127.1, 90.5, and 67.6 mg/cm$^2$, respectively, and the thickness of the oxide layer decreases from 882 to 441 μm. Obviously, the antioxidant performance of the sample increases gradually with the increase in B content. The fracture toughness of the alloy increases first and then decreases, while the microhardness of Nbss increases slightly with the increase in B content. Furthermore, Zhang et al. [4] also studied the synergistic effects of B, Hf, and Cr, and the results showed that the synergy of B and Cr had a better oxidation resistance, while the addition of Hf was not conducive to enhancing the oxidation resistance of the alloy. The fracture toughness of the alloy decreases with the addition of B, while the macroscopic hardness does not change significantly. Moreover, in the work of Thomas et al. [30], the effect of different Si and B content (at %) on the oxidation resistance of Nb-25Cr-15Mo-xSi-yB alloy was studied (hereinafter, it is abbreviated as xSi-yB alloy). The oxidation products of 20Si-10B and 20Si-15B (at.%) alloys are mainly $CrNbO_4$ and $SiO_2$. The weight gain of 20Si-15B alloy is the minimum at 1200 and 1400 °C, while the weight gain of 15Si-15B alloy is the minimum at 900 °C, which may be attributed to the occurrence of pest oxidation and the spalling of the oxide layer, as shown in **Figure 11**. Therefore, the high content of Si and B is more beneficial to enhance the oxidation resistance of the Nb alloys. Moreover, the research of Su et al. [31] shows that the synergy of B and Ge can facilitate the production of continuous and dense oxide film in the alloy and reduce the penetration rate of $O_2$. It is worth noting that the dissolution of $B_2O_3$ and $GeO_2$ in silicide can also improve the TEC of the oxide scales and make it more compatible with the substrate so as to suppress the occurrence of cracks and improve the oxidation life of the alloy.

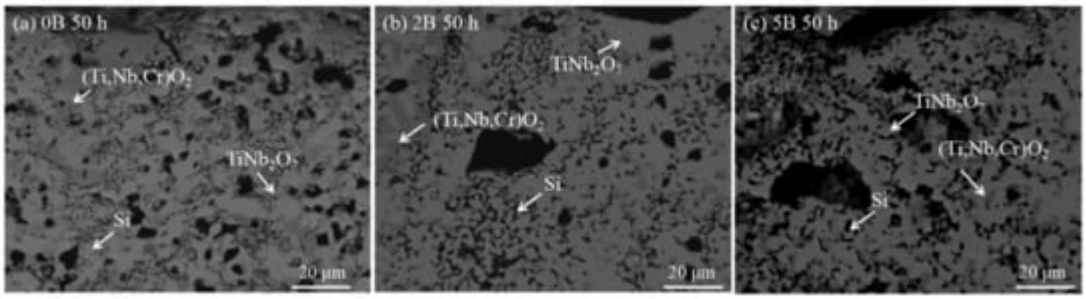


**Figure 10.** Cross-sectional BSE images of the Nb-22Ti-16Si-5Cr-4Hf-3Al-xB (x = 0 at.%, 2 at.%, 5 at.%) alloys after oxidation at 1250 °C: (**a**) 0B, (**b**) 2B, and (**c**) 5B. Copyright 2014 Elsevier.

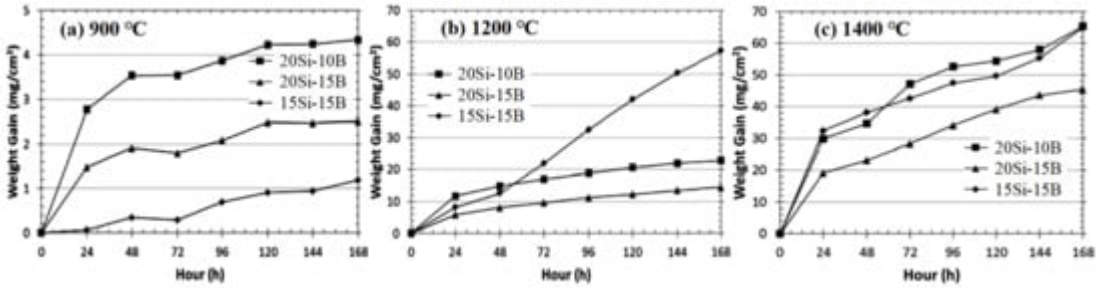


**Figure 11.** Long-term oxidation curves for alloys at (**a**) 900 °C, (**b**) 1200 °C, and (**c**) 1400 °C. Copyright 2015 Elsevier.

## References


1. Geng, J.; Tsakiropoulos, P.; Shao, G.S. Oxidation of Nb-Si-Cr-Al in situ composites with Mo, Ti and Hf additions. Mater. Sci. Eng. A 2006, 441, 26–38.
2. Geng, J.; Tsakiropoulos, P. A study of the microstructures and oxidation of Nb-Si-Cr-Al-Mo in situ composites alloyed with Ti, Hf and Sn. Intermetallics 2007, 15, 382–395.
3. Vazquez, A.; Varma, S.K. High-temperature oxidation behavior of Nb-Si-Cr alloys with Hf additions. J. Alloys Compd. 2011, 509, 7027–7033.
4. Zhang, S.; Guo, X. Alloying effects on the microstructure and properties of Nb–Si based ultrahigh temperature alloys. Intermetallics 2016, 70, 33–44.
5. Zhang, S.; Guo, X.P. Microstructure, mechanical properties and oxidation resistance of Nb silicide based ultrahigh temperature alloys with Hf addition. Mater. Sci. Eng. A 2015, 645, 88–98.
6. Cui, K.K.; Zhang, Y.Y.; Fu, T.; Hussain, S.; AlGarni, T.S.; Wang, J.; Zhang, X.; Ali, S. Effects of Cr2O3 content on microstructure and mechanical properties of Al2O3 substrate composites. Coatings 2021, 11, 234.
7. Pan, Y. Structural Prediction and overall performances of CrSi2 disilicides: DFT investigations. ACS Sustain. Chem. Eng. 2020, 8, 11024–11030.
8. Chan, K.S. Cyclic oxidation response of multiphase niobium-based alloys. Met. Mater. Trans. A 2004, 35, 589–597.
9. Wang, L.G.; Jia, L.N.; Cui, R.J.; Zheng, L.L.; Zhang, H. Microstructure, mechanical properties and oxidation resistance of Nb-22Ti-14Si-2Hf-2Al-xCr alloys. Chin. J. Aeronaut. 2012, 25, 292–296.
10. Zelenitsas, K.; Tsakiropoulos, P. Study of the role of Al and Cr additions in the microstructureof Nb-Ti-Si in situ composites. Intermetallics 2005, 13, 1079–1095.
11. Zelenitsas, K.; Tsakiropoulos, P. Effect of Al, Cr and Ta additions on the oxidation behaviour of Nb-Ti-Si in situ composites at 800 °C. Mater. Sci. Eng. A 2006, 416, 269–280.

12. Esparza, N.; Rangel, V.; Gutierrez, A.; Arellano, B.; Varma, S.K. A comparison of the effect of Cr and Al additions on the oxidation behaviour of alloys from the Nb–Cr–Si system. Mater. High Temp. 2016, 33, 105–114.
13. Zhang, S.; Guo, X. Effects of Cr and Hf additions on the microstructure and properties of Nb silicide based ultrahigh temperature alloys. Mater. Sci. Eng. A 2015, 638, 121–131.
14. Pan, Y.; Pu, D.; Yu, E. Structural, electronic, mechanical and thermodynamic properties of Cr–Si binary silicides from first-principles investigations. Vacuum 2021, 185, 110024.
15. Su, L.; Jia, L.; Jiang, K.; Zhang, H. The oxidation behavior of high Cr and Al containing Nb-Si-Ti-Hf-Al-Cr alloys at 1200 and 1250 °C. Int. J. Refract. Met. Hard Mater. 2017, 69, 131–137.
16. Tsai, Y.L.; Wang, S.F.; Bor, H.Y.; Hsu, Y.F. Effects of Zr addition on the microstructure and mechanical behavior of a fine-grained nickel-based superalloy at elevated temperatures. Mater. Sci. Eng. A 2014, 607, 294–301.
17. Luo, C.; Lu, N.; Zhu, C.L.; Li, H.Z.; Liu, X.Q. Effect of trace zirconium addition on high temperature mechanical properties of casting TiAl alloy. Foundry 2012, 61, 754–757.
18. Swadźba, R.; Swadźba, L.; Wiedermann, J.; Hetmańczyk, M.; Witala, B. Characterization of alumina scales grown on a 2nd generation single crystal Ni superalloy during isothermal oxidation at 1050, 1100 and 1150 °C. Oxid. Met. 2014, 82, 195–208.
19. Hong, S.; Hwang, G.; Han, W.; Lee, K.; Kang, S. Effect of zirconium addition on cyclic oxidation behavior of platinum-modified aluminide coating on nickel-based superalloy. Intermetallics 2010, 18, 864–870.
20. Zhang, S.-N.; Jia, L.-N.; Guo, Y.; Kong, B.; Zhang, F.-X.; Zhang, H. High-temperature oxidation behavior of Nb–Si-based alloy with separate vanadium, tantalum, tungsten and zirconium addition. Rare Met. 2021, 40, 607–615.
21. Zhang, S.; Jia, L.; Guo, Y.; Kong, B.; Zhou, C.; Zhang, H. Improvement in the oxidation resistance of Nb-Si-Ti based alloys containing zirconium. Corros. Sci. 2020, 163, 108294.
22. Qiao, Y.; Guo, X.; Zeng, Y. Study of the effects of Zr addition on the microstructure and properties of Nb-Ti-Si based ultrahigh temperature alloys. Intermetallics 2017, 88, 19–27.
23. Ma, R.; Guo, X. Composite alloying effects of V and Zr on the microstructures and properties of multi-elemental Nb–Si based ultrahigh temperature alloys. Mater. Sci. Eng. A 2021, 813, 141175.
24. Behrani, V.; Thom, A.J.; Kramer, M.J.; Akinc, M. Microstructure and oxidation behavior of Nb-Mo-Si-B alloys. Intermetallics 2006, 14, 24–32.
25. Zhang, Y.Y.; Cui, K.K.; Fu, T.; Wang, J.; Shen, F.Q.; Zhang, X.; Yu, L.H. Formation of MoSi2 and Si/MoSi2 coatings on TZM (Mo-0.5Ti-0.1Zr-0.02C) alloy by hot dip silicon-plating method. Ceram. Int. 2021, 47, 23053–23065.

26. Wu, M.L.; Jiang, L.W.; Qu, S.Y.; Guo, F.W.; Li, M.; Kang, Y.W.; Han, Y.F. Effect of trace Ce and B additions on the microstructure of Nb-3Si-22Ti alloys. Prog. Nat. Sci. Mater. Int. 2017, 27, 362–368.
27. Zhang, Y.Y.; Li, Y.G.; Bai, C.G. Microstructure and oxidation behavior of Si-MoSi2 functionally graded coating on Mo substrate. Ceram. Int. 2017, 43, 6250–6256.
28. Zhang, S.; Guo, X. Effects of B addition on the microstructure and properties of Nb silicide based ultrahigh temperature alloys. Intermetallics 2015, 57, 83–92.
29. Sun, Z.; Guo, X.; Guo, B. Effect of B and Ti on the directionally solidified microstructure of the Nb–Si alloys. Int. J. Refract. Met. Hard Mater. 2015, 51, 243–249.
30. Thomas, K.S.; Varma, S.K. Oxidation response of three Nb-Cr-Mo-Si-B alloys in air. Corros. Sci. 2015, 99, 145–153.
31. Su, L.F.; Jia, L.N.; Weng, J.F.; Hong, Z.; Zhou, C.G.; Zhang, H. Improvement in the oxidation resistance of Nb-Ti-Si-Cr-Al-Hf alloys containing alloyed Ge and B. Corros. Sci. 2014, 88, 460–465.